24th COBEM - 2017

24th ABCM International Congress of Mechanical Engineering
December 3-8, 2017, Curitiba, PR, Brazil

COBEM-2017-0274
BOUNDARY INTEGRAL SOLUTION OF SOUND PROPAGATION AND SCATTERING IN NON-UNIFORM POTENTIAL FLOWS WITH A NUMERICAL GREEN'S FUNCTION

Simone Mancini
Victor Rosa
ISVR, University of Southampton, UK
vhprosa@me.com

Abstract. *Sound propagation in moving media can be solved using a boundary integral formulation to the limit of weakly non-uniform potential flows. For low Mach numbers, an approximate analytical Green's function can be found as a combination of the physical models associated with the Taylor and Lorentz transforms. A boundary element method can then be used to solve scattering of sound by solid surfaces in a mean flow. These solutions, however, deteriorate with increasing Mach number and frequency. In this work, we compute a numerical Green's function to assess the error of the approximate analytical Green's function. It is shown that the numerical Green's provides only minor improvements to the solutions based on the analytical Green's function. It is concluded that the analytical Green's function is a good approximation of the exact one.*

Keywords: *sound propagation, sound scattering, non-uniform flows, boundary element method.*

1. INTRODUCTION

The effect of aircraft noise on the environment is a main concern for the aviation industry and research institutes. There is an impelling need of fast numerical methods to predict aircraft noise sources and the corresponding installation effects during design cycles (Balin *et al.*, 2016). Particularly for aeronautical applications, the problem involves sound with short wave length propagating for long distances and through non-uniform flows. For example, the sound generated by the fan in the engine radiates from the engine intake initially through a non-uniform flow, then reaches the aircraft fuselage where it is scattered, and finally propagates for long distances before reaching the far-field observer.

For such problems, volume-based methods such as finite element methods (Astley and Eversman, 1981), discontinuous Galerkin methods (Gabard, 2007) and high order finite difference schemes (Tam and Webb, 1993) can compute propagation of sound through non-uniform mean flow by solving the linearised Euler equations. But these methods are too computationally expensive for use in the design phase of large-scale aircraft in the case of high-frequency sound propagation problems (Astley, 2009).

Boundary element methods (BEM) coupled with fast algorithms, such as the fast multipole method (Gumerov and Duraiswami, 2004) or the H-Matrix algorithm (Hackbusch, 1999), can solve large-scale short-wavelength noise propagation around aircraft (Balin *et al.*, 2016). On the other hand, a boundary element formulation which solves either the linearised Euler equations or the full potential linearised wave equation is yet to be provided—BEM needs a boundary integral solution and the corresponding Green's function. At the moment, BEM is limited to solve approximate formulations for non-uniform mean flow (Astley and Bain, 1986; Tinetti and Dunn, 2005).

Non-uniform mean flow effects have been included in boundary element solutions using variable transformations in order to reduce the approximate wave operator with mean flow to the Helmholtz problem (Tinetti and Dunn, 2005; Clancy, 2010; Wolf and Lele, 2013; Mayoral and Papamoschou, 2013). Mancini *et al.* (2016a,b) proposed a formulation in the physical space, i.e. without transformation, to solve a low-Mach-number approximation of the full potential linearised wave equation (Astley, 1985) with small non-uniform Mach numbers—this equation has been referred to as the weakly non-uniform flow wave equation. Physical-space solutions have the advantage that sound sources and boundary conditions are written in their natural, physical, form.

In this paper, we solve the weakly non-uniform flow wave equation presented by Mancini *et al.* (2016a) using a finite element approach. Unlike the boundary element solution proposed by Mancini *et al.* (2016a), for which an approximate analytical Green's function has been used, in the present work solutions based on finite elements will provide results accounting for exact Green's function. The goal of the paper is, therefore, to show that the analytical Green's function is a good approximation to solve the weakly non-uniform flow wave equation.

The structure of the paper is as follows. In Section 2, the physical model is reviewed. In Section 3, the boundary integral solution is discussed. In Section 4, a weak formulation for the weakly non-uniform flow wave equation is presented. In Section 5, numerical examples are provided. Conclusions are given in Section 6.

2. PHYSICAL MODEL

We want to solve external sound propagation and scattering in a non-uniform subsonic potential mean flow (see Figure 1). An inviscid, homentropic, irrotational and steady flow is considered as a base flow and acoustic perturbations are assumed to be of small amplitude compared with the base flow. Wave propagation on a non-uniform mean flow can then be written for a potential formulation as (Astley, 1985),

$$\frac{D_0}{Dt}\left(\frac{\rho_0}{c_0^2}\frac{D_0\hat{\phi}}{Dt}\right) - \boldsymbol{\nabla}\cdot\left(\rho_0\boldsymbol{\nabla}\hat{\phi}\right) = 0, \tag{1}$$

where $\hat{\phi}(\mathbf{x},t)$ is the acoustic velocity potential and $D_0/Dt = \partial/\partial t + \mathbf{u}_0\cdot\nabla$ denotes the material derivative over the mean flow. ρ_0 is the mean flow density, c_0 the speed of sound and $\mathbf{u}_0$ the mean flow velocity.

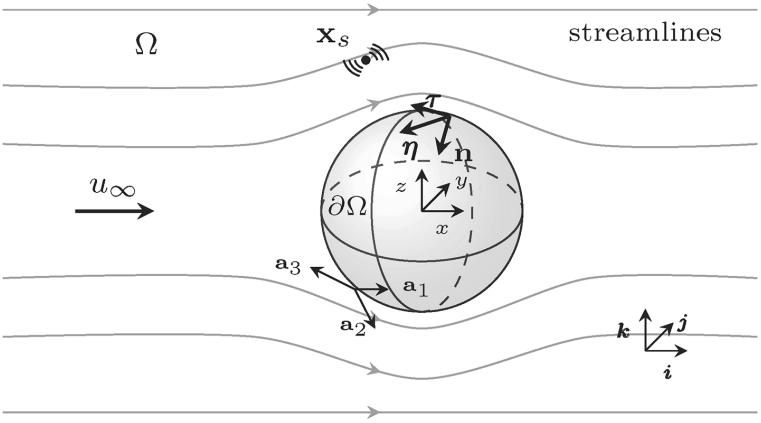

Figure 1. Sketch of the geometrical features for sound propagation and scattering in a potential flow.

Equation (1) can be simplified considering the dependence of the formulation on the mean flow Mach number M_∞, the acoustic and mean flow length scales, L_A and L_M respectively. Here the acoustic length scale is the wavelength, and the mean flow length scale is the distance in which the mean flow has changed significantly (say, the distance from the stagnation point to where the velocity magnitude is $\approx 0.99M_\infty$). The simplifications amount to retain only terms of order $[\phi]/L_A^2$, $M_\infty[\phi]/L_A^2$, $M_\infty^2[\phi]/L_A^2$ and assume that $L_A \leq L_M$ for $M_\infty \ll 1$. Moreover, the mean flow is decomposed in a uniform and a non-uniform component $\mathbf{u_0} = \mathbf{u}_\infty + \mathbf{u}_\mathbf{0}'$ and it assumed that that non-uniform component is small compared with the uniform flow part ($\mathbf{u}_\mathbf{0}' \ll \mathbf{u}_\infty$). The resulting simplified formulation for a general three-dimensional incoming mean flow - but limiting, for simplicity, the free-stream mean flow velocity to be parallel to the x-axis - is as (Clancy, 2010; Mancini *et al.*, 2016a)

$$\frac{1}{c_\infty^2}\frac{\partial^2\hat{\phi}}{\partial t^2} + \frac{2}{c_\infty^2}\mathbf{u}_0\cdot\boldsymbol{\nabla}\frac{\partial\hat{\phi}}{\partial t} - \nabla^2\hat{\phi} + \frac{u_\infty^2}{c_\infty^2}\frac{\partial^2\hat{\phi}}{\partial x^2} = 0, \tag{2}$$

where u_∞ is the uniform flow velocity aligned with the x-axis. Equation (2) has been referred to as the weakly non-uniform potential flow wave equation (Mancini *et al.*, 2016a). It has been obtained assuming $M_0' \ll M_\infty$ and $M_\infty \ll 1$, meaning that $M_0'M_\infty \ll M_\infty^2$ and $M_0'^2 \ll M_\infty^2$, where he Mach number $\mathbf{M_0}(\mathbf{x}) = \mathbf{u_0}(\mathbf{x})/c_\infty = \mathbf{M}_\infty + \mathbf{M}_0'(\mathbf{x})$.

In this work, a harmonic problem is solved, i.e. $\hat{\phi} = \phi e^{i\omega t}$, where ϕ is a complex number. Equation (2) can be written in frequency domain as

$$k^2\phi - 2ik\mathbf{M}_0\cdot\boldsymbol{\nabla}\phi + \nabla^2\phi - M_\infty^2\frac{\partial^2\phi}{\partial x^2} = 0, \tag{3}$$

where $k = \omega/c_\infty$. Equation (3) is solved in this work, either using a finite element approach or a boundary integral formulation. The problem is solved in an unbounded domain, so that Sommerfeld radiation condition with mean flow must be satisfied for $\mathbf{x} \to \infty$.

3. BOUNDARY INTEGRAL SOLUTION

An integral solution to Eq. (3) at any collocation point $\mathbf{x}_p$, either in Ω or on the boundary surface $\partial\Omega$ (see Figure 1), has been presented by Mancini *et al.* (2016a) as

$$\hat{C}(\mathbf{x}_p)\phi(\mathbf{x}_p) = \int_{\partial\Omega}\left[G\left(\frac{\partial\phi}{\partial n} - \frac{\partial\phi}{\partial x}n_x M_\infty^2\right) - \phi\left(\frac{\partial G}{\partial n} - \frac{\partial G}{\partial x}n_x M_\infty^2\right) - 2\mathrm{i}k\mathbf{M}_0\cdot\mathbf{n}\phi G\right]dS + \phi_{inc}, \tag{4}$$

where $G = G(\mathbf{x}_p, \mathbf{x})$, $\phi = \phi(\mathbf{x})$ and $\phi_{inc} = \phi_{inc}(\mathbf{x}_p)$ is a generic incident field. In the above equation, $\mathbf{n}(\mathbf{x})$ is the outgoing normal vector to the boundary surface and

$$\hat{C}(\mathbf{x}_p) = \begin{cases} 1 & \mathbf{x}_p \in \Omega \\ 0 & \mathbf{x}_p \notin \Omega \cup \partial\Omega \\ 1 - \int_{\partial\Omega}\left[\frac{\partial G_0}{\partial n} - M_\infty^2\frac{\partial G_0}{\partial x}n_x\right]dS & \mathbf{x}_p \in \partial\Omega. \end{cases} \tag{5}$$

Note that $G_0(\mathbf{x}_p, \mathbf{x})$ is the free-field Green's function for the static problem $\nabla^2 G_0 + M_\infty^2\partial^2 G_0/\partial x^2 = \delta(\mathbf{x} - \mathbf{x}_p)$. The incident field $\phi_{inc}(\mathbf{x}_p)$ and the Green's function $G(\mathbf{x}_p, \mathbf{x})$ were written by Mancini *et al.* (2016a), respectively, as

$$\phi_{inc}(\mathbf{x}_p) = \int_\Omega G(\mathbf{x}_p, \mathbf{x})g(\mathbf{x})dV \qquad \text{and} \qquad G(\mathbf{x}_p, \mathbf{x}) = \frac{\mathrm{e}^{-\mathrm{i}k\sigma_M}}{4\pi R_M}, \tag{6}$$

where $\sigma_M = [R_M + M_\infty(x_p - x)]/\beta_\infty^2 + [\Phi_0'(\mathbf{x}_p) - \Phi_0'(\mathbf{x})]/c_\infty$ is the generalized reverse flow phase radius, $R_M = \sqrt{(x_p - x)^2 + \beta_\infty^2[(y_p - y)^2 + (z_p - z)^2]}$, $\beta_\infty = \sqrt{1 - M_\infty^2}$ and Φ_0' the non-uniform part of the mean flow velocity potential. For a 2D problem the corresponding Green's function can be written as

$$G(\mathbf{x}_p, \mathbf{x}) = -\frac{\mathrm{i}}{4\beta_\infty}H_0^{(2)}\left(\frac{kR_{M,2D}}{\beta_\infty^2}\right)\exp\left[-\mathrm{i}k\left(\frac{M_\infty(x_p - x)}{\beta_\infty^2} + \frac{\Phi_0'(\mathbf{x}_p) - \Phi_0'(\mathbf{x})}{c_\infty}\right)\right], \tag{7}$$

where $R_{M,2D} = \sqrt{(x - x_s)^2 + \beta_\infty^2(y - y_s)^2}$.

4. WEAK FORMULATION

A limitation of solving Eq. (4) is that the Green's function (see Eqs. (6) and (7)) neglects terms of order $M_0' M_\infty$ and $M_0'^2$ - or higher - consistent with the weakly non-uniform ansatz. To overcome this limitation, a finite element model can be solved. Equation (3) can be written for a generic sound source, g, as

$$k^2\phi - 2\mathrm{i}k\mathbf{M}_0\cdot\nabla\phi + \nabla^2\phi - M_\infty^2\frac{\partial^2\phi}{\partial x^2} = g, \tag{8}$$

A weak formulation of the above equation can be written for an incompressible flow as

$$\begin{aligned}&\int_\Omega\left[\psi k^2\phi - \psi\mathrm{i}k\mathbf{M}_0\cdot\nabla\phi + \phi\mathrm{i}k\mathbf{M}_0\cdot\nabla\psi - \nabla\psi\cdot\nabla\phi + M_\infty^2\frac{\partial\phi}{\partial x}\frac{\partial\psi}{\partial x}\right]dV = \\ &-\int_{\partial\Omega}\psi\left[\nabla\phi\cdot\mathbf{n} - M_\infty^2\frac{\partial\phi}{\partial x}n_x - \mathrm{i}k\mathbf{M}_0\cdot\mathbf{n}\phi\right]dS + \int_\Omega\psi g dV,\end{aligned} \tag{9}$$

where ψ is a complex test function. Note that the third term of the surface integral on the right-hand side of the above equation vanishes for a stationary surface. Nonetheless, the term $\nabla\phi\cdot\mathbf{n}$ vanishes for rigid surfaces.

Equation (9) can be discretised, and a linear system of equations solved using a finite element approach. Although an equivalent solution can be given for the full potential linearised wave equation, solving the above equation is relevant to the present work - solving the weakly non-uniform flow wave equation allows the solution for the exact Green's function to be computed in lieu of the solution based on the approximate Green's function, Eq. (4).

5. NUMERICAL RESULTS

5.1 Numerical model

We solve the scattering of sound by an infinite cylinder (see Figure 2). The objective of the present numerical experiment is to compare a solution to the weakly non-uniform flow formulation with an exact Green's function with the

solution based on an approximated analytical Green's function. The scope of the numerical analysis is as follows. First, we compute the finite element solution based on the weakly non-uniform flow formulation, Eq. (9). This finite element solution is sampled on a closed surface including the source and the scattering body. The solution on the surface is then extrapolated using the boundary integral solution in Eq. (4).

The solutions are then compared with the solution of the full potential linearised wave equation (Astley, 2009), Eq. (1), which is taken as the reference solution. We also compute the solution of the convected wave equation, i.e. assuming only a uniform flow in the domain, which is currently the most common formulation used in industrial boundary element applications (Balin *et al.*, 2015).

In this case, the sound field is generated by a volume point source and scattered by the infinite cylinder of radius a, as shown in Figure 2. A potential incompressible mean flow is computed solving Laplace's equation and imposed as base flow. The sound source is a harmonic monopole volume point source,

$$\hat{g}(\mathbf{x}, t) = \delta(\mathbf{x} - \mathbf{x}_0)\mathrm{e}^{\mathrm{i}\omega t}. \tag{10}$$

A nodal point is defined at the source location and the mesh is refined in its neighbourhood so that 20 elements with quadratic interpolation contribute to the source nodal point.

The problem is solved in the frequency domain. The radiation condition, in the FE solution, is satisfied using a perfect matching layer (Bermudez *et al.*, 2007). On the other hand, the radiation condition is inherently satisfied by the boundary integral formulation and the Green's function.

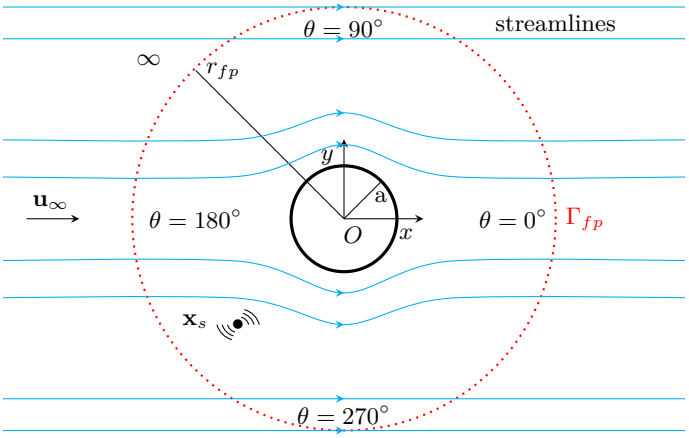

Figure 2. Sketch of the geometrical features for sound propagation and scattering around a cylinder. The dotted line denotes an arc of field points.

The evaluation of the accuracy of a numerical solution can be based, e.g., on the physical model, representation of the geometry, mean flow interpolation, interpolation error and source representation. In this analysis, the focus is on the physical model. The solutions are compared both in terms of acoustic potential, ϕ, and pressure, p'. The acoustic potential is the field variable used to describe the model, while the acoustic pressure, p', can be recovered from the linearised momentum equation,

$$p' = -\rho_0(\mathrm{i}\omega\phi + \mathbf{u}_0 \cdot \nabla\phi). \tag{11}$$

Note that an analytical derivative of the Green's function is performed to recover the gradient of the potential, $\nabla\phi$, in the boundary element solution, whereas the derivative is performed numerically for the reference finite element solution. In other words, in the finite element solution the pressure is one order of interpolation lower in accuracy than the acoustic potential. This drawback is mitigated by mesh refinement.

The error analyses is computed as the Euclidean norm:

$$E_{L^2} = \sqrt{\frac{\int_{\Gamma_{fp}} \|\chi - \chi_{ref}\|^2 dS}{\int_{\Gamma_{fp}} \|\chi_{ref}\|^2 dS}}, \tag{12}$$

where χ is the numerical solution, χ_{ref} the reference value, and Γ_{fp} is the surface along which the values are sampled. The L^2-error is used to measure the accuracy of the physical model, compared with that of reference, i.e. the full potential linearised wave equation.

However, other sources of error will inevitably be present in the solution. The truncation of the physical domain in the FE solution and the application of a perfect matching layer create spurious reflections. Moreover, the exact and the

discrete wavenumbers differ. This results in the dispersion error which propagates and accumulates in the discrete FE domain, causing the so-called pollution effect (Babuška and Sauter, 1997; Bériot *et al.*, 2013). By using eight degrees of freedom per wavelength, quadratic element interpolation and truncating the domain in the acoustic and geometrical far field, these errors are reasonably controlled.

Nonetheless, solutions based on wave extrapolation will be affected by interpolation error. The finite element solutions in the inner domain are sampled on a control surface where the acoustic potential and its derivatives are recovered based on the discrete solution. Although the nodal points of the discrete control surface and finite element grid are chosen to coincide, $\nabla\phi$ must be recovered numerically from the finite element solution in the inner domain.

Figures 3 and 4 show contours of the real part of the acoustic velocity potential at $M_\infty = 0.3$ and a non-dimensional wavenumber $ka = 3\pi$. Finite element solutions of the full potential linearised wave equation (LPE), Eq. (1), and the weakly non-uniform flow formulation (WNUF), Eq. (3), are shown along with solution to the weakly non-uniform flow formulation including wave extrapolation. The solutions are shown for two source locations: in Figure 3 a source downstream the cylinder, at $\mathbf{x}_s = (1.5a, 0)$; and in Figure 4 a source to the side of the cylinder, at $\mathbf{x}_s = (0, 1.5a)$.

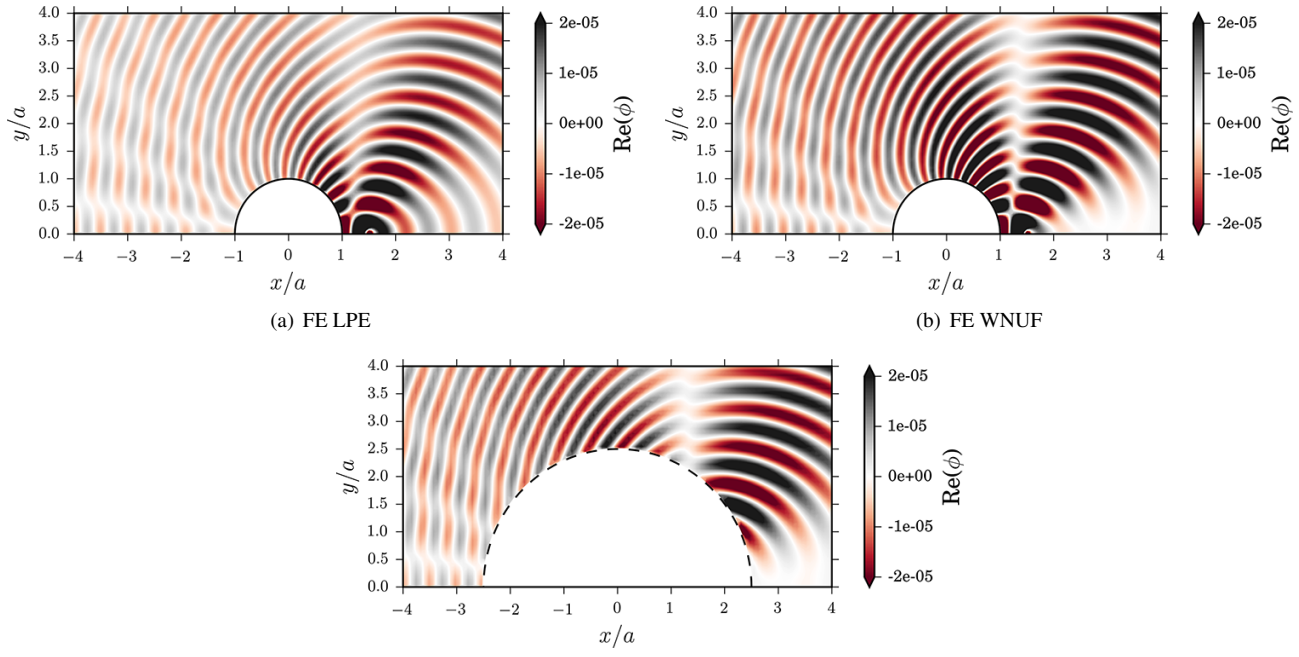

(a) FE LPE

(b) FE WNUF

(c) WNUF extrapolated

Figure 3. Contours of the real part of the acoustic velocity potential ϕ for the problem in Figure 2 at $M_\infty = 0.3$ and $ka = 3\pi$ with $\mathbf{x}_s = (1.5a, 0)$.

5.2 Effect of wave extrapolation radius

In this section, the impact of using the exact Green's function on the numerical results is assessed. The improvements brought by the exact Green's function in comparison with the approximate analytical Green's function are assessed by using a wave extrapolation approach. Radiation and scattering around the cylinder in an inner domain is solved using Eq. (9). Then the solution is sampled on a radiating surface. The radius of the wave extrapolation surface is varied. The different radii are chosen in order extrapolate waves either from a non-uniform or a uniform mean flow. Note that Eq. (4) is exact whenever the acoustic field is extrapolated in a uniform flow.

We consider the problem with the source at $\mathbf{x}_s = (0, 1.5a)$. The radius of the collocation points, where the error is computed, is fixed at $8a$, whereas the radius for the extrapolation takes the following values: $2.5a$, $4a$, and $7a$. The problem is solved at $ka = 2\pi$ and $ka = 4\pi$—these non-dimensional wavenumbers represent a wavelength of half and quarter of the cylinder, respectively. A finite element solution of LPE is used as reference solution. In Figure 5, the L^2-error is shown at M_∞ in the range 0.1–0.3.

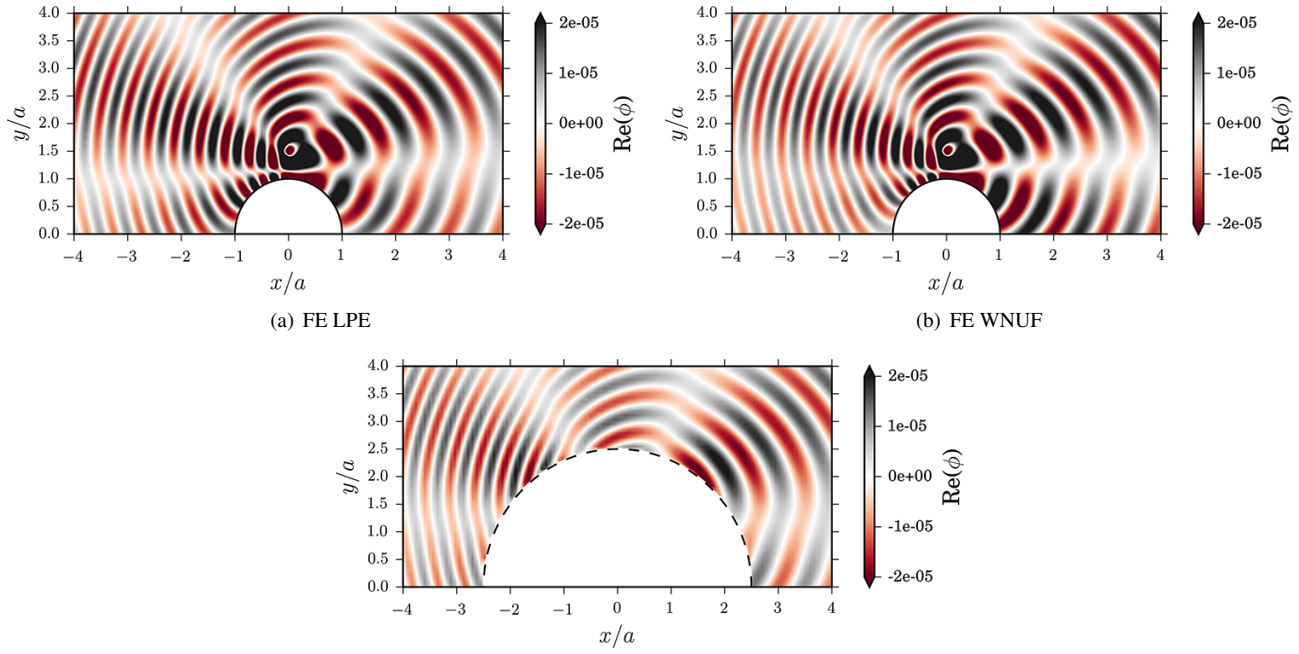

(a) FE LPE

(b) FE WNUF

(c) WNUF extrapolated

Figure 4. Contours of the real part of the acoustic velocity potential ϕ, for the problem in Figure 2 at $M_\infty = 0.3$ and $ka = 3\pi$ with $\mathbf{x}_s = (0, 1.5a)$.

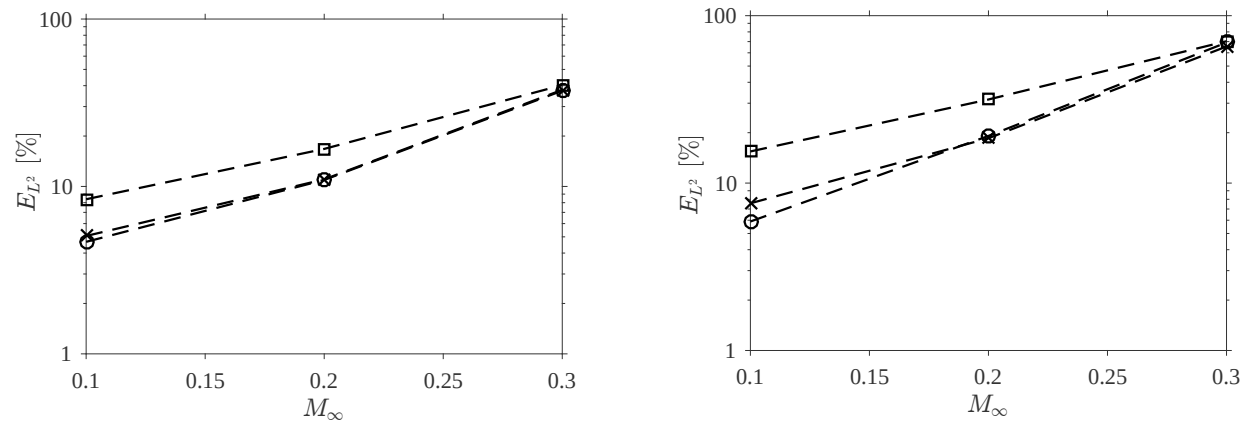

(a) $ka = 2\pi$

(b) $ka = 4\pi$

Figure 5. L^2-error for the wave extrapolated solutions and the problem in Figure 2 with sound source at $\mathbf{x}_s = (0, 1.5a)$. Error computed against the reference LPE solution along an arc of field point with radius $8a$. The extrapolation radii are 2.5a (□), 4a (×) and 7a (△).

Figure 5 shows that the error increases with Mach number. The error decreases with an increase of the radius of the surface from which the acoustic field is extrapolated. The error increases when the extrapolation surface is closer to the region where the flow non-uniformities are higher, i.e. closer to the cylinder. In the limit of a boundary element formulation, the problem would be solved up to the boundary surface, further increasing the error. The error of the numerical Green's function can be reduced by increasing the radius of the extrapolation surface. Yet, the improvement provided by increasing the radius of the surface of extrapolation is almost negligible at $M_\infty = 0.3$. We can conclude that at $M_\infty = 0.3$ the error is mostly due to the inaccuracy of the approximate physical model, i.e. the weakly non-uniform flow formulation, rather than the approximate Green's function.

5.3 Effect of source location

In this section, we assess the effect of source location for cases with a free-stream Mach number of $M_\infty = 0.3$. The non-dimensional wavenumber is varied from $ka = \pi$ to $ka = 5\pi$. Two sources location are considered: (i) downstream the cylinder, at $\mathbf{x}_s = (1.5a, 0)$; and (ii) to the side of the cylinder, at $\mathbf{x}_s = (0, 1.5a)$. Figure 6 shows the L^2-error against the

non-dimensional quantity ka/π at a circular arc of field points with radius $r = 8a$. We compare the solutions provided by using the finite element formulation for either the convected Helmholtz equation, i.e. considering only a uniform flow, the corresponding solution based on the weakly non-uniform flow formulation and the solution based on wave extrapolation with $r = 2.5a$.

It is shown that the solution of the convected Helmholtz equation leads to the largest error. However, it is comparable to the error from the extrapolated solution for the downstream source and $ka = 5\pi$. Note that the weakly non-uniform flow has been shown to decrease accuracy with increase in frequency (Mancini *et al.*, 2016a). The error shown by the full FE solution of the weakly non-uniform flow is slightly smaller than that generated by the extrapolated solution in the case of the downstream source location while it is comparable to it for the other source location.

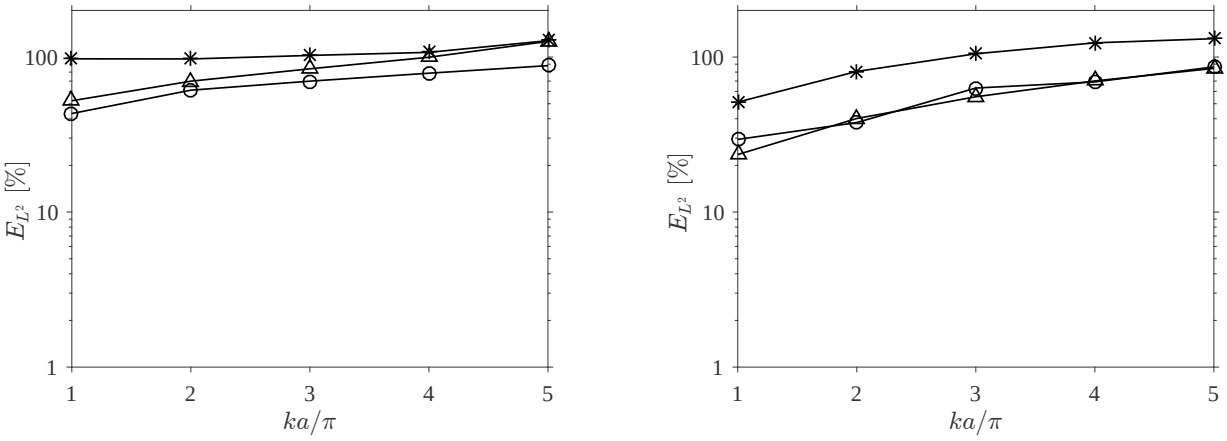

(a) $\mathbf{x}_s = (0, 1.5a)$ (b) $\mathbf{x}_s = (1.5a, 0)$

Figure 6. L^2-error for the wave extrapolated solutions and the problem in Figure 2 at $M_\infty = 0.3$ and sound source at $\mathbf{x}_s$. Error computed against the reference LPE solution along an arc of field point with radius $8a$. The extrapolation radii is 2.5a. FE convected wave equation (*), FE weakly non-uniform flow and wave extrapolation with radius 2.5a ($\triangle$) and FE weakly non-uniform flow ($\circ$).

5.4 Directivity and phase

We now compare the results from different formulations. In this case, we compute sound pressure level (SPL) and phase of the acoustic pressure field. The SPL is computed as

$$\mathrm{SPL} = 20 \log_{10} \left(\frac{p'_{rms}}{p'_{ref}} \right), \tag{13}$$

in which the reference pressure is $p'_{ref} = 2 \cdot 10^{-5}$ Pa, and $p'_{rms} = \|p'\|/\sqrt{2}$.

Figure 7 compares the sound pressure levels along an arc of field points with radius $r = 8a$. The results are provided for $M_\infty = 0.3$ and a non-dimensional frequency of $ka = 3\pi$. The SPL is shown for two different position of the sound source, i.e. $\mathbf{x}_s = (1.5a, 0)$ and $\mathbf{x}_s = (0, 1.5a)$. The corresponding results in terms of phase of the acoustic pressure field are shown in Figure 8.

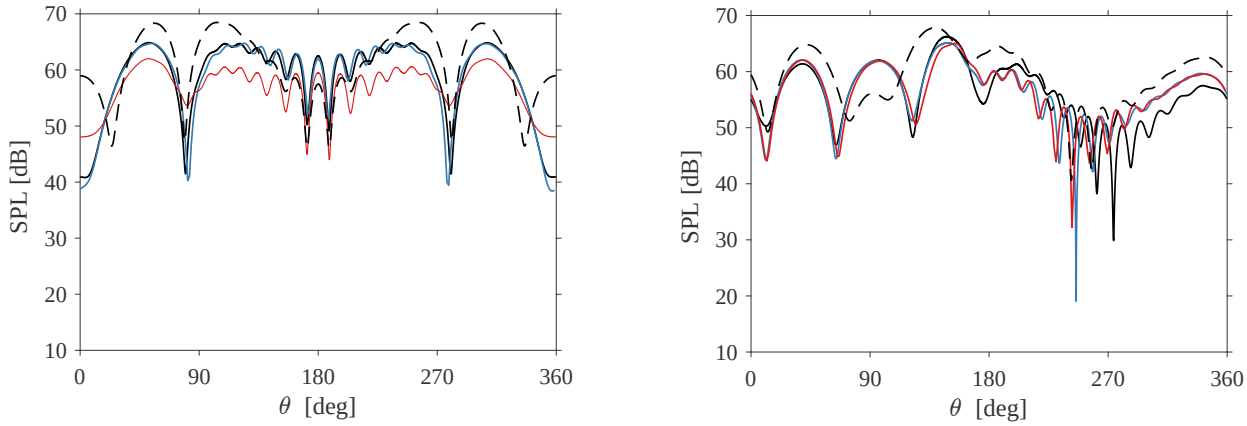

(a) downstream source (b) side source

Figure 7. SPL along a circular arc of field points with radius $r = 8a$ at $ka = 3\pi$. (a) Downstream source at $\mathbf{x}_s = (1.5a, 0)$, (b) side source at $\mathbf{x}_s = (0, 1.5a)$. Black lines, FE solution of LPE; black dashed lines, FE solution of convected Helmholtz equation; blue lines FE solution of WNUF; red lines WNUF solution with approximate Green's function (extrapolation for $r = 2.5a$).

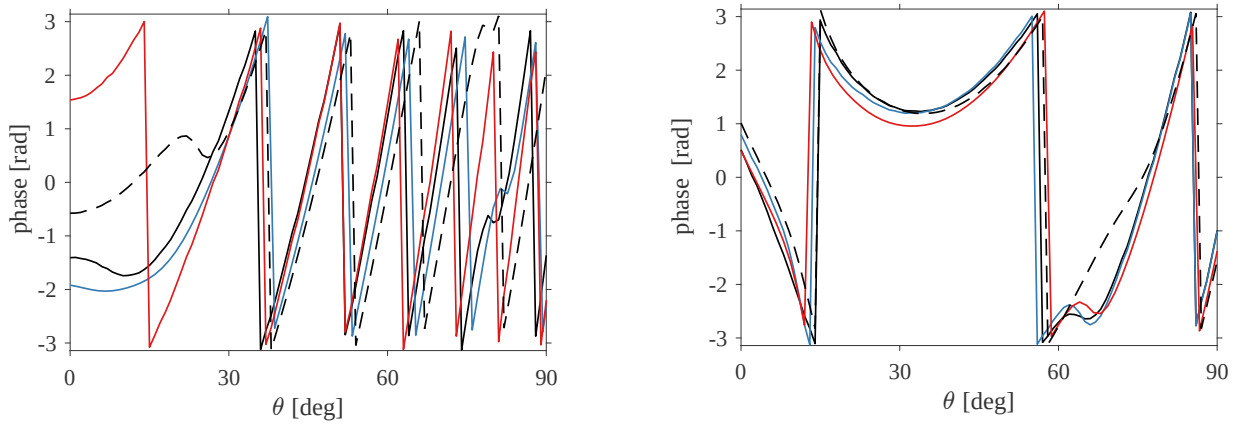

(a) $\mathbf{x}_s = (1.5a, 0)$ (b) $\mathbf{x}_s = (0, 1.5a)$

Figure 8. Phase of the acoustic pressure field along a circular arc of field points with radius $r = 8a$ at $ka = 3\pi$. (a) Downstream source at $\mathbf{x}_s = (1.5a, 0)$, (b) side source at $\mathbf{x}_s = (0, 1.5a)$. For line colours, refer to the caption in Figure 7.

The results indicate that the uniform flow approximation is the most inaccurate formulation. The results based on the weakly non-uniform flow formulation are in good agreement. The difference between these formulations, i.e. based on either the exact or the approximated Green's function, is much smaller than the difference shown with the full potential linearised wave equation. Differences up to 8 dB are shown compared with the LPE, in the worst-case scenario, i.e. for the downstream source location.

6. CONCLUSIONS

This paper assessed the possibility to improve the boundary element solution of the weakly non-uniform flow formulation presented by Clancy (2010) and Mancini *et al.* (2016a). The possible improvements were sought in the approximations of the Green's function used by Mancini *et al.* (2016a).

An exact Green's function, computed numerically by a finite element approach, was used to work around the error generated by the approximations of the analytical Green's function. Solutions based on the numerical Green's function were computed either up to a uniform flow or in a inner domain in order to provide the solution in a non-uniform flow region and extrapolate to the far field based on the approximate analytical Green's function.

Using a numerical Green's function, however, was not the long-term goal of this work. Solutions based on the numerical Green's function were recovered in order to benchmark the analytical Green's function. The numerical Green's function showed only minor improvements of the solution, confirming that the analytical Green's function is a good approximation for the solution of the weakly non-uniform flow wave equation. In particular the improvement provided by

the exact Green's function is much smaller than the difference observed with the finite element solution of the reference physical model, i.e. the linearised potential wave equation.

7. ACKNOWLEDGEMENTS

The first author thanks Prof. Jeremy R. Astley and Dr. Gwénaël Gabard for the discussions from which this work has been carried out. The second author acknowledges financial support from the CAPES agency of the Brazilian Ministry of Education.

8. REFERENCES

Astley, R.J., 2009. "Numerical methods for noise propagation in moving flows, with application to turbofan engines". *Acoust. Sci. & Tech.*, Vol. 30, pp. 227–239.

Astley, R.J. and Eversman, W., 1981. "Acoustic transmission in lined ducts with flow, part 2: the finite element method". *J. Sound Vib.* , Vol. 74, pp. 103–121.

Astley, R., 1985. "A finite element, wave envelope formulation for acoustical radiation in moving flows". *J. Sound Vib.* , Vol. 3, pp. 471–485.

Astley, R. and Bain, J., 1986. "A 3D boundary element scheme for acoustic radiation in low Mach number". *J. Sound and Vib.*, Vol. 109, No. 1, pp. 445–465.

Babuška, I. and Sauter, S., 1997. "Is the pollution effect of the fem avoidable for the helmholtz equation considering high wave numbers?" *SIAM J. Numer. Anal.*, Vol. 34, No. 6, pp. 2392–2423.

Balin, N., Casenave, F., Dubois, F., Duceau, E., Duprey, S. and Terrasse, I., 2015. "Boundary element and finite element coupling for aeroacoustics simulations". *J. Comput. Phys.*, Vol. 294, pp. 274–296.

Balin, N., Sylvand, G. and Robert, J., 2016. "Fast methods applied to BEM solvers for acoustic propagation problems". Lyon, France, number AIAA 2016-2712 in 22nd AIAA/CEAS Aeroacoustics Conference.

Bériot, H., Gabard, G. and Perrey-Debain, E., 2013. "Analysis of high-order finite elements for convected wave propagation". *Int. J. Numer. Meth. Eng.*, Vol. 96, No. 11, pp. 665–688.

Bermudez, A., Hervella-Nieto, L., Prieto, A. and Rodriguez, R., 2007. "An optimal perfectly matched layer with unbounded absorbing function for time-harmonic acoustic scattering problems". *J. Comput. Phys.*, Vol. 223, No. 2, pp. 469–488.

Clancy, C., 2010. *Boundary Element methods for the prediction of aircraft noise shielding in flight*. Ph.D. thesis, University of Dublin, Dep. of Mechanical and Manufacturing Eng.

Gabard, G., 2007. "Discontinuous galerkin methods with plane waves for time-harmonic problems". *J. Comput. Phys.*, Vol. 225, No. 2, pp. 1961–1984.

Gumerov, A. and Duraiswami, R., 2004. *Fast Multipole Methods for Helmholtz Equation in Three Dimensions*. Elsevier, London.

Hackbusch, W., 1999. "A sparse matrix arithmetic based on H-matrices. part I: Introduction to H-matrices". *Computing*, Vol. 62, No. 2, pp. 89–108.

Mancini, S., Astley, R., Sinayoko, S., Gabard, G. and Tournour, M., 2016a. "An integral formulation for wave propagation on weakly non-uniform potential flows". *J. Sound Vib.*, Vol. 385, pp. 184–201.

Mancini, S., Sinayoko, S., Astley, R., Gabard, G. and Tournour, M., 2016b. "Boundary element formulation for wave propagation in weakly non-uniform potential flows". Lyon, France, number AIAA 2016-2713 in 22nd AIAA/CEAS Aeroacoustics conference.

Mayoral, S. and Papamoschou, D., 2013. "Prediction of jet noise shielding with forward flight effects". Grapevine, Texas, number AIAA 2013-0010 in 51st Aerospace Science Meeting.

Tam, C. and Webb, J., 1993. "Dispersion-relation-preserving finite difference schemes for computational acoustics". *J. Comput. Phys.*, Vol. 107, pp. 262–281.

Tinetti, A. and Dunn, M., 2005. "Aeroacoustic noise prediction using the fast scattering code". Monterey, California, number AIAA 2005-3061 in 11th AIAA/CEAS Aeroacoustics Conference.

Wolf, W.R. and Lele, S.K., 2013. "Fast acoustic scattering predictions with non-uniform potential flow effects". *J. Braz. Soc. Mech. Sci*, Vol. 35, No. 4, pp. 407–418.

9. RESPONSIBILITY NOTICE

The authors are the only responsible for the printed material included in this paper.